Supporting Information

Mapping the working route of phosphate monoester hydrolysis catalyzed by copper based models with special emphasis on the role of oxoanions by experimental and theoretical studies

Sanchari Dasgupta,[a] Gabriel Aullón,*[b] Ennio Zangrando[c] and Debasis Das*[a]

[a]Department of Chemistry, University of Calcutta, 92 A.P.C Road, Kolkata:700009, India
[b]Departament de Química Inorgànica i Orgànica (Secció de Química Inorgànica) and Institut de QuímicaTeorica i Computacional, Universitat de Barcelona , Martí i Franques 1-11, 08028 Barcelona, Spain
[c]Department of Chemical and Pharmaceutical Sciences,University of Trieste,Via L. Giorgieri 1, 34127 Trieste, Italy

Contents of Supporting Information

1) **Fig. S1** FT-IR spectrum of complex **2**
2) **Fig. S2** FT-IR spectrum of complex **3**
3) **Fig. S3** UV-Vis spectra of complexes **2** and **3** in DMF medium
4) **Table S1** Coordination Bond Lengths (Å) and Angles (°) for Complex **2**
5) **Table S2** Coordination Bond Lengths (Å) and Angles (°) for Complex **3**
6) **Fig. S4** Intramolecular and Intermolecular H-bonding interactions operative between two tetranuclear units of complex **2**
7) **Fig. S5** Polymeric network of complex **2** viewed along crystallographic axis *a* propagated via H-bonding interactions
8) **Fig. S6** Intramolecular and intermolecular H-bonding interactions operative between two tetranuclear units of complex **3** via lattice water molecule
9) **Fig. S7** Polymeric network of complex **3** viewed along crystallographic axis *a* propagated via H-bonding interactions
10) **Fig. S8** ESI-MS spectrum of comple**x 2** in acetonitrile medium
11) **Fig. S9** ESI-MS spectrum of complex **3** in acetonitrile medium
12) **Fig. S10** Controlled experiment of Phosphatase activity for ligand H_2L in 97.5% DMF-H_2O mixture
13) **Fig. S11** Controlled experiment of Phosphatase activity for $[Cu(ClO_4)_2]$ in 97.5% DMF-H_2O mixture

14) **Fig. S12** Controlled experiment of Phosphatase activity for [$Cu(NO_3)_2$] in 97.5% DMF-H_2O mixture
15) **Fig. S13** Controlled experiment of Phosphatase activity for [$Cu(OAc)_2$] in 97.5% DMF-H_2O mixture
16) **Table S3** First-order rate parameters for phosphatase activity as obtained by the non linear treatment of Michaelis-Menten treatment of complexes **1**, **2** and **3**
17) **Fig. S14** Plot of enzymatic kinetics of hydrolysis of 4-NPP for (a) complex **1**, (b) complex **2** and (c) complex **3**
18) **Fig. S15** ESI-MS spectrum of reaction mixture of complex **2** and 4-NPP recorded in positive mode
19) **Fig. S16** ESI-MS spectrum of reaction mixture of complex **3** and 4-NPP recorded in positive mode
20) **Table S4** Relative Gibbs Free Energies in DMF Solution for Compounds Involved in the Reaction Shown in the Scheme 2 Having Symmetrically Disposition of Bischelate Ligand L. The Energy for Initial Complexes is Arbitrarily Taken to Zero. All Energies are in kJ/mol
21) **Table S5** Main Geometric Parameters for the Optimized Binuclear Structures. Distances in Angstroms, Angles in Degrees
22) **Table S6** Continous Shape Measures (CSM) for Copper Atoms in the Computed Geometries Accross the Proposed Pathway
23) **Table S7** Crystallographic Data and Details of Refinements for Complexes **2** and **3**

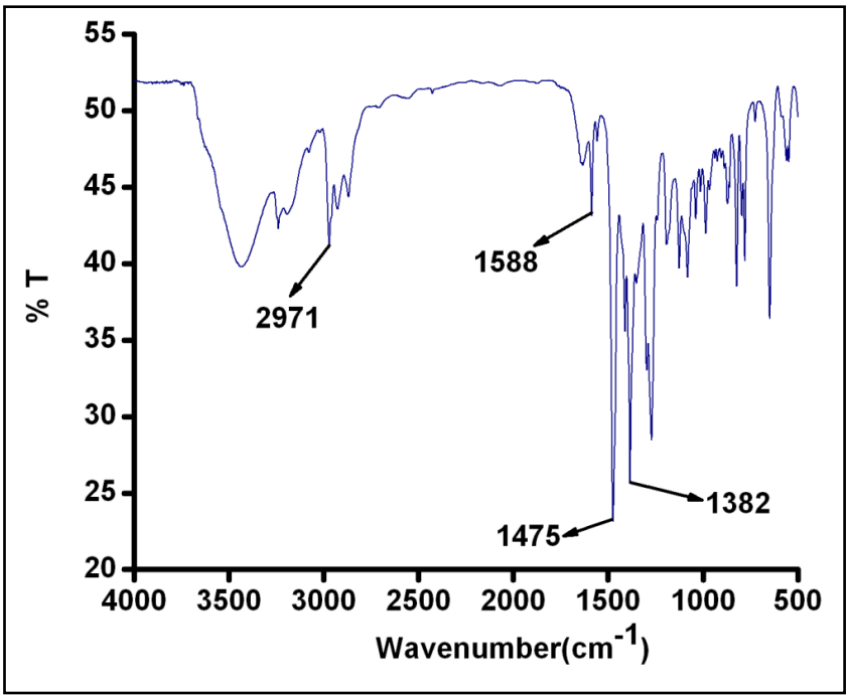

Fig. S1 FT-IR spectrum of complex **2**.

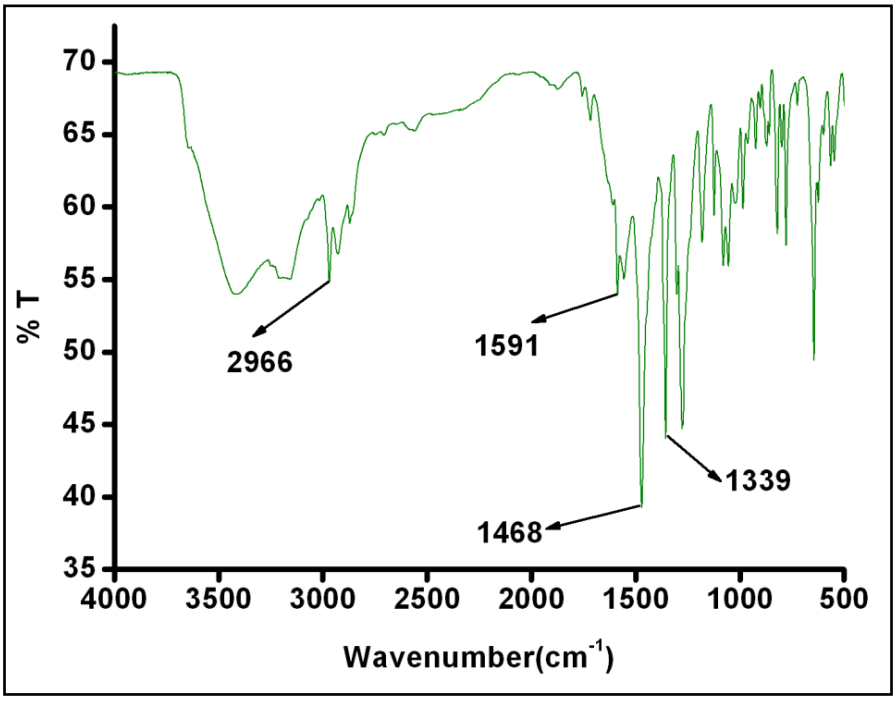

Fig. S2 FT-IR spectrum of complex **3**.

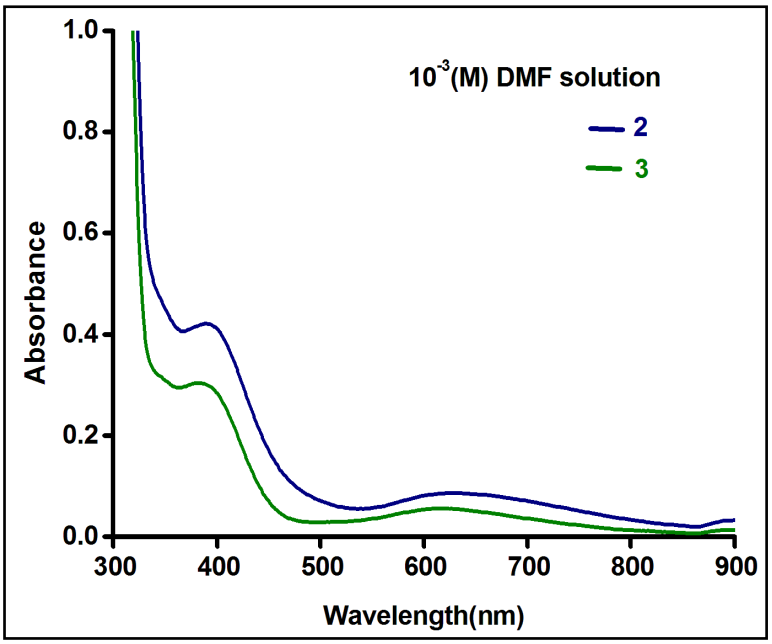

Fig. S3 UV-Vis spectra of complexes **2** and **3** in DMF medium.

Table S1 Coordination bond lengths (Å) and angles (°) for complex **2**

Cu(1)-O(1)	1.921(5)	Cu(2)-O(3)	1.907(5)
Cu(1)-N(1)	1.985(6)	Cu(2)-N(2)	1.972(6)
Cu(1)-O(2)	1.973(5)	Cu(2)-O(4)	1.926(5)
Cu(1)-O(4)	1.907(5)	Cu(2)-O(1)	2.094(5)
Cu(1)-O(5)	2.355(7)	Cu(2)-O(3')	2.172(5)
Cu(1)-Cu(2)	2.9735(14)	Cu(2)-Cu(2')	3.131(2)

O(1)-Cu(1)-N(1)	95.5(2)	O(3)-Cu(2)-N(2)	96.5(2)
N(1)-Cu(1)-O(2)	84.4(2)	N(2)-Cu(2)-O(4)	84.7(2)
O(4)-Cu(1)-O(1)	83.7(2)	O(3)-Cu(2)-O(4)	178.5(2)
O(4)-Cu(1)-N(1)	171.4(3)	O(3)-Cu(2)-O(3')	79.9(2)
O(4)-Cu(1)-O(2)	95.3(2)	O(4)-Cu(2)-O(3')	98.6(2)
O(1)-Cu(1)-O(2)	173.0(2)	N(2)-Cu(2)-O(3')	126.3(2)
O(1)-Cu(1)-O(5)	92.0(3)	O(3)-Cu(2)-O(1)	100.7(2)
O(2)-Cu(1)-O(5)	95.0(3)	O(4)-Cu(2)-O(1)	78.8(2)
O(4)-Cu(1)-O(5)	93.5(2)	N(2)-Cu(2)-O(1)	141.1(2)
N(1)-Cu(1)-O(5)	95.0(3)	O(3')-Cu(2)-O(1)	91.1(2)

Primed atoms at -x+1,-y,-z+1

Table S2 Coordination bond lengths (Å) and angles (°) for complex **3**.

Cu(1)-O(1)	1.927(3)	Cu(2)-O(3)	1.925(3)
Cu(1)-N(1)	1.983(4)	Cu(2)-N(2)	1.997(4)
Cu(1)-O(2)	2.013(3)	Cu(2)-O(4)	1.928(3)
Cu(1)-O(4)	1.905(3)	Cu(2)-O(1)	2.061(3)
Cu(1)-O(5)	2.279(4)	Cu(2)-O(3')	2.214(3)
Cu(1)-Cu(2)	2.9936(8)	Cu(2)-Cu(2')	3.1996(12)

O(1)-Cu(1)-N(1)	94.74(14)	O(3)-Cu(2)-N(2)	95.25(14)
N(1)-Cu(1)-O(2)	84.18(14)	N(2)-Cu(2)-O(4)	84.11(14)
O(4)-Cu(1)-O(1)	81.64(13)	O(3)-Cu(2)-O(4)	179.36(13)
O(4)-Cu(1)-N(1)	160.01(16)	O(3)-Cu(2)-O(3')	78.95(13)
O(4)-Cu(1)-O(2)	97.67(14)	O(4)-Cu(2)-O(3')	101.39(13)
O(1)-Cu(1)-O(2)	174.87(15)	N(2)-Cu(2)-O(3')	124.61(14)
O(1)-Cu(1)-O(5)	96.88(14)	O(3)-Cu(2)-O(1)	102.81(13)
O(2)-Cu(1)-O(5)	88.24(14)	O(4)-Cu(2)-O(1)	77.73(13)
O(4)-Cu(1)-O(5)	101.80(14)	N(2)-Cu(2)-O(1)	142.72(15)
N(1)-Cu(1)-O(5)	98.15(15)	O(3')-Cu(2)-O(1)	91.04(13)

Primed atoms at -x+1,-y+1,-z+1

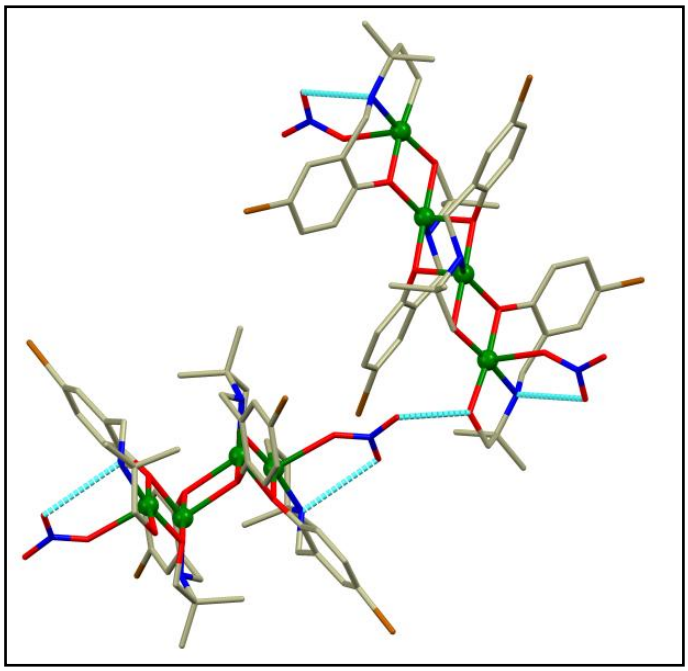

Fig. S4 Intramolecular and Intermolecular H-bonding interactions operative between two tetranuclear units of complex **2**.

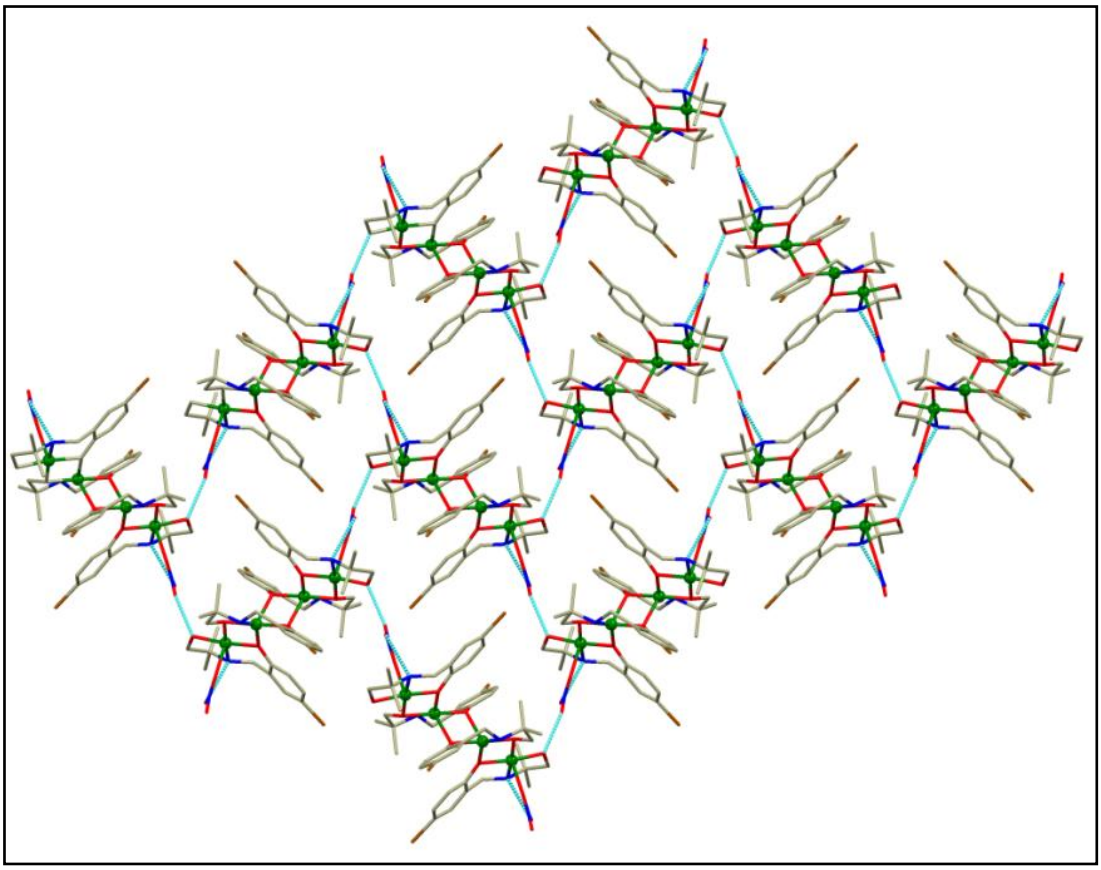

Fig. S5 Polymeric network of complex **2** viewed along crystallographic axis *a* propagated via H-bonding interactions.

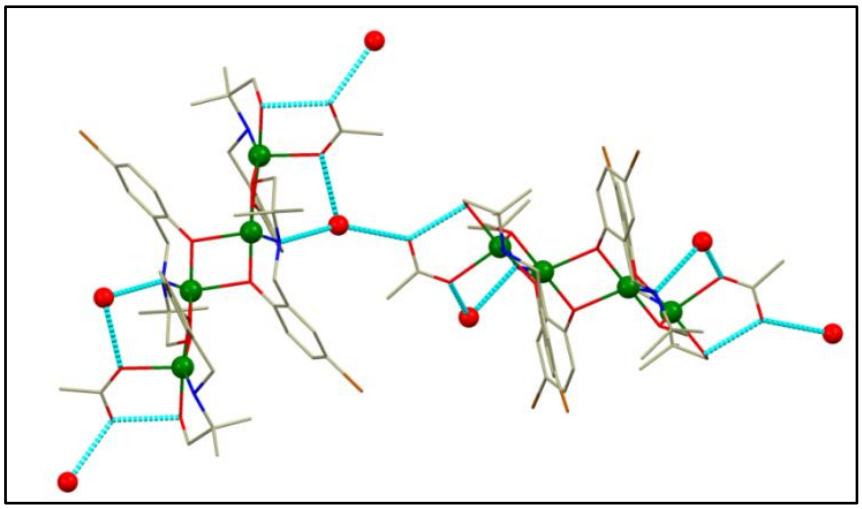

Fig. S6 Intramolecular and intermolecular H-bonding interactions operative between two tetranuclear units of complex **3** via lattice water molecule.

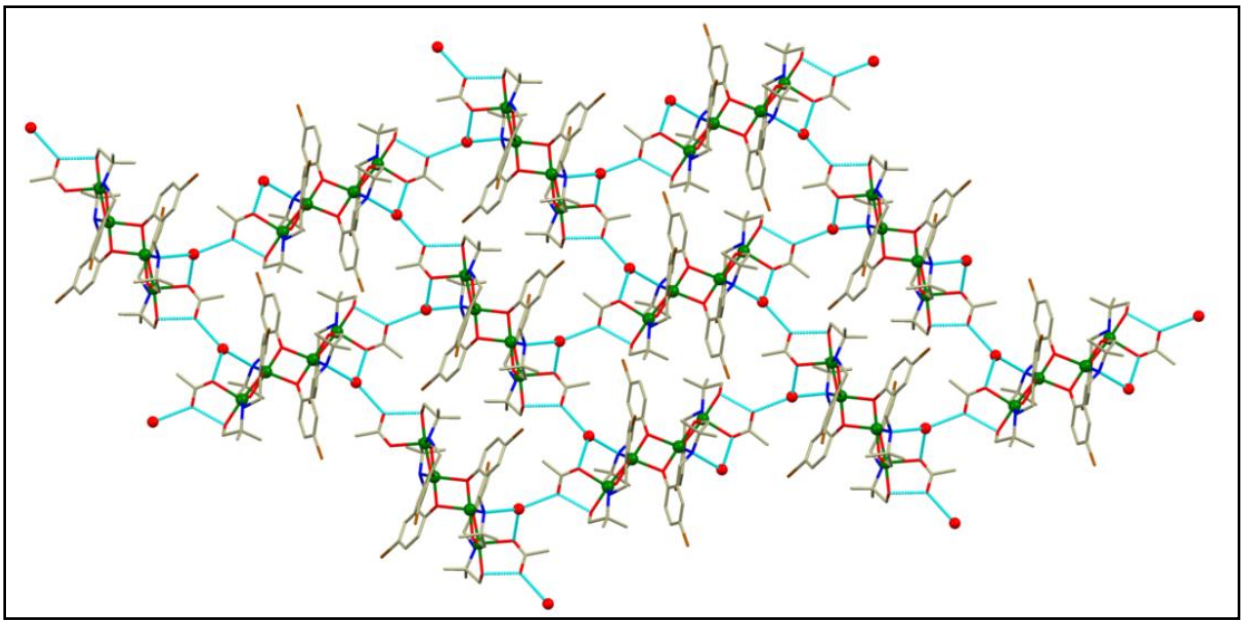

Fig. S7 Polymeric network of complex **3** viewed along crystallographic axis *a* propagated via H-bonding interactions.

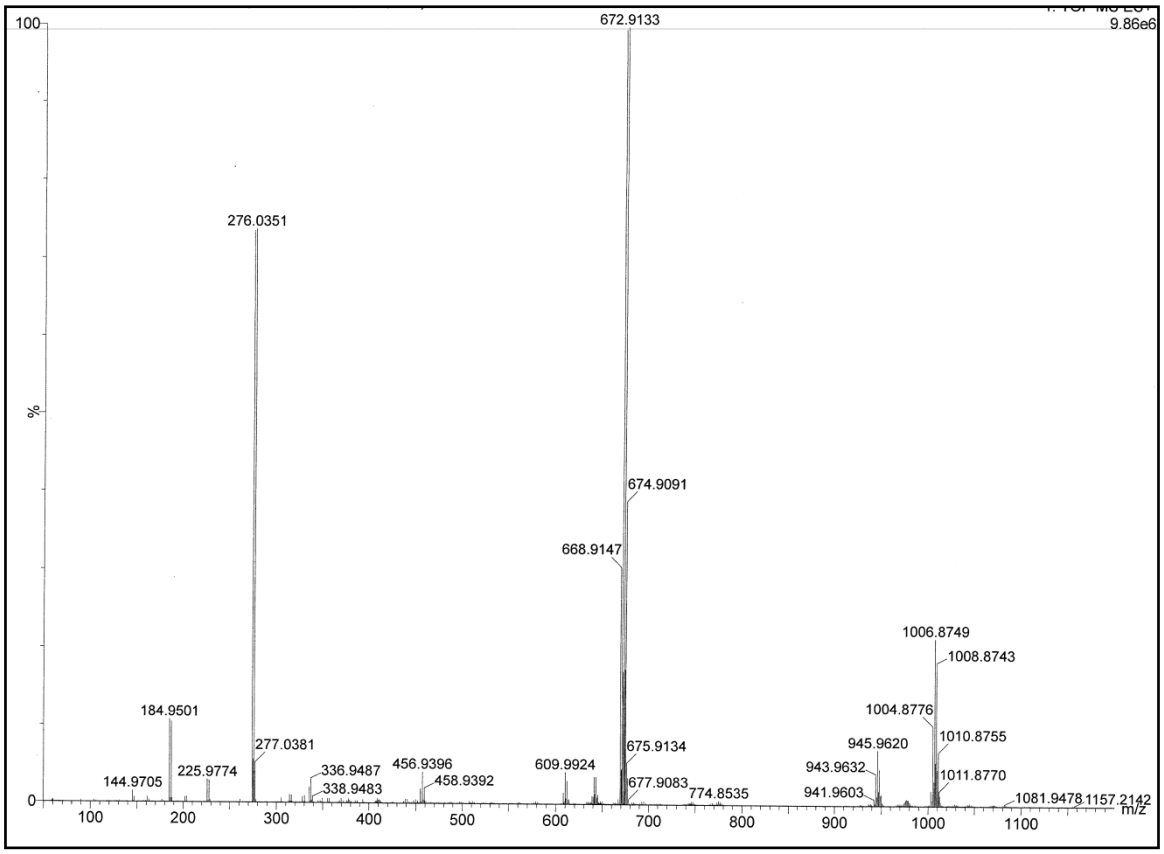

Fig. S8 ESI-MS spectrum of complex **2** in acetonitrile medium.

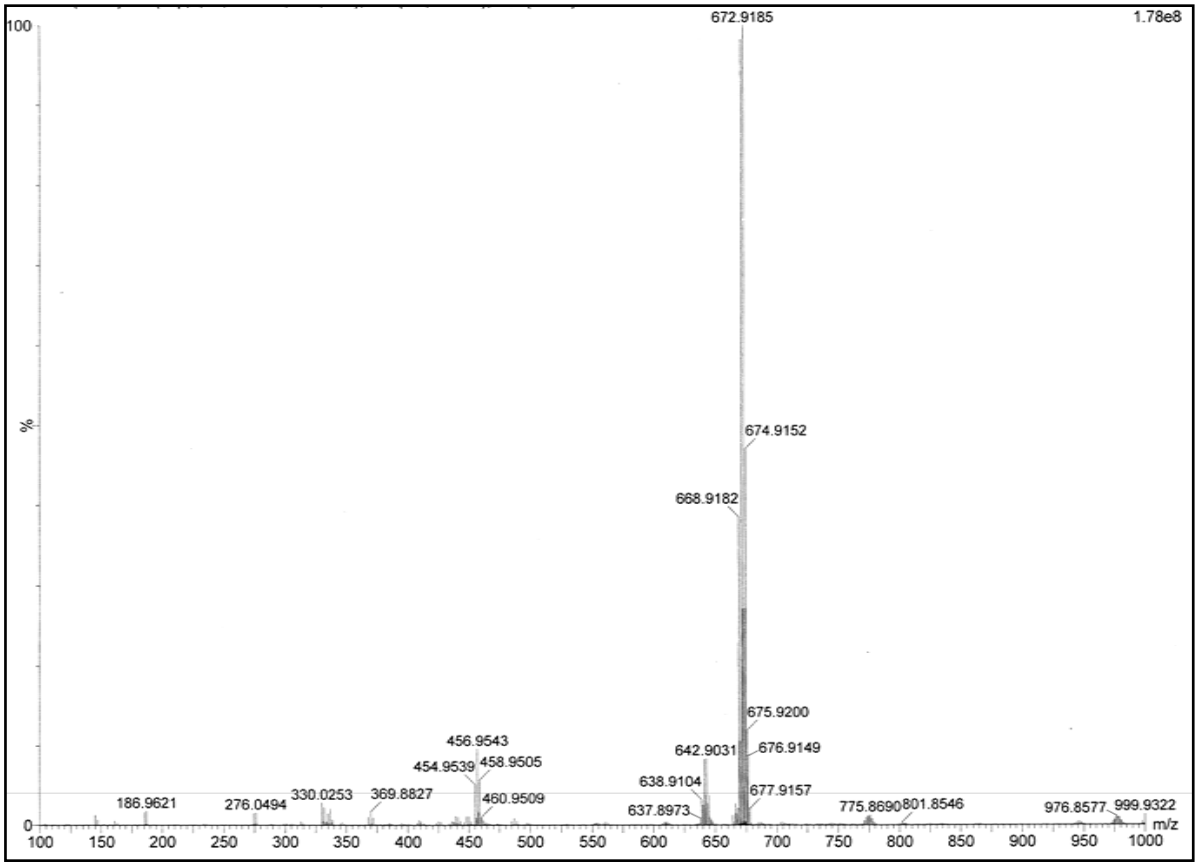

Fig. S9 ESI-MS spectrum of complex **3** in acetonitrile medium.

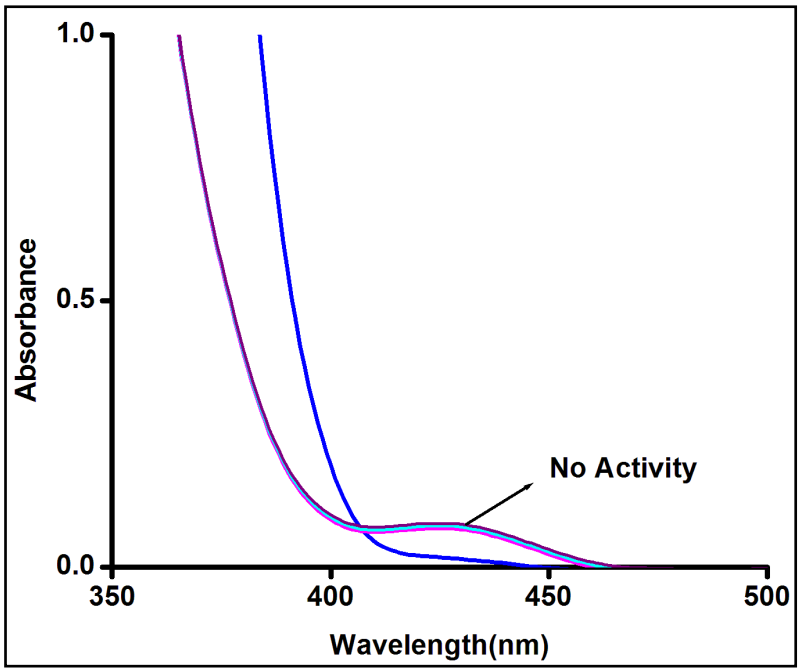

Fig. S10 Controlled experiment of Phosphatase activity for ligand **H_2L** in 97.5% DMF-H_2O mixture.

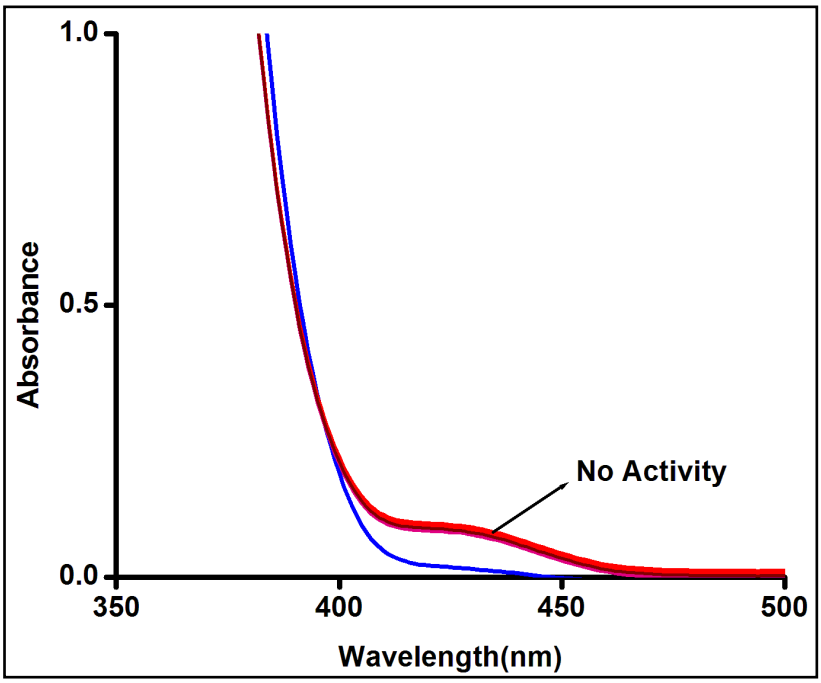

Fig. S11 Controlled experiment of Phosphatase activity for $[Cu(ClO_4)_2]$ in 97.5% DMF-H_2O mixture .

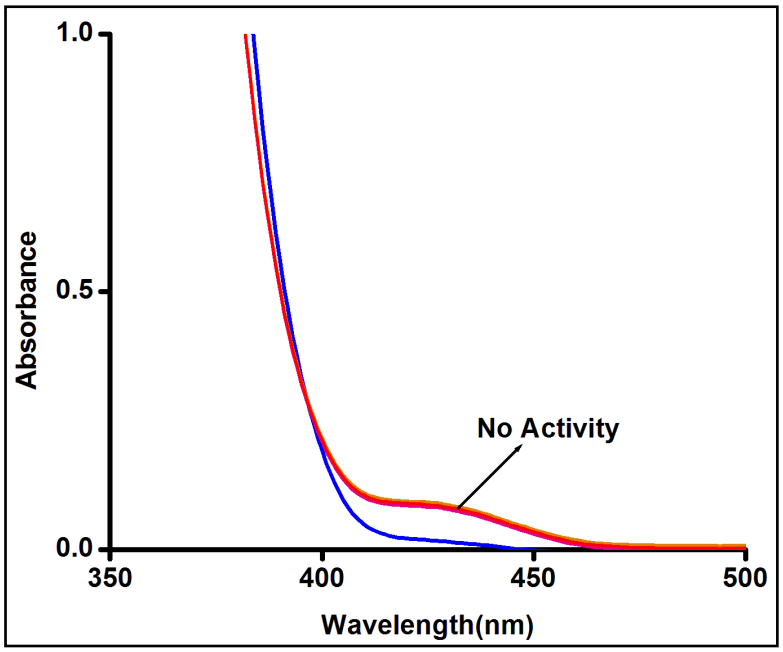

Fig. S12 Controlled experiment of Phosphatase activity for $[Cu(NO_3)_2]$ in 97.5% DMF-H_2O mixture .

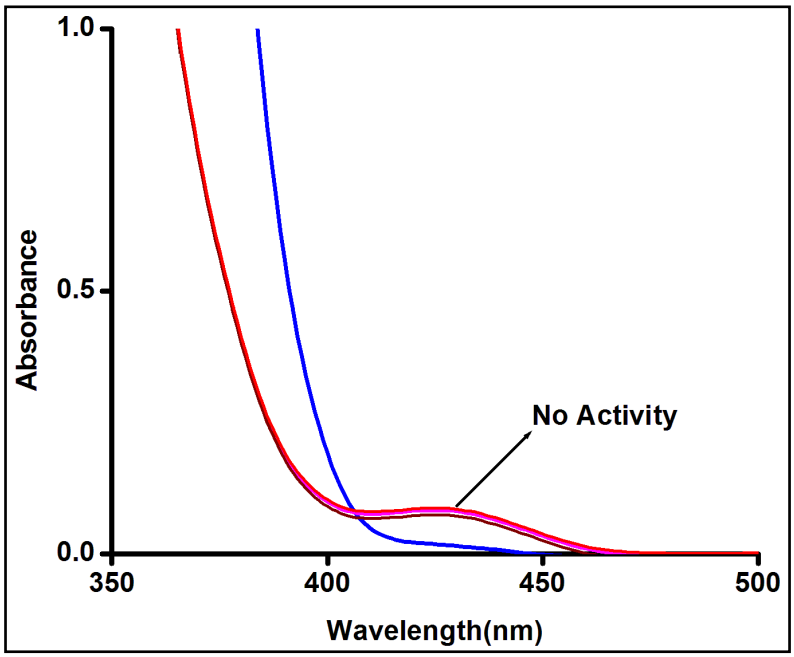

Fig. S13 Controlled experiment of Phosphatase activity for $[Cu(OAc)_2]$ in 97.5% DMF-H_2O mixture .

Table S3 First-order rate parameters for phosphatase activity as obtained by the non linear treatment of Michaelis-Menten treatment of complexes **1**, **2** and **3**

Complex	**V_{max} (M s^{-1})**	**K_M (M)**	**k_{cat} (s^{-1})**	**k_{cat}/ K_M(M^{-1} s^{-1})**	**Std. Error**
Complex **1**	4.526×10^{-4}	1.43×10^{-3}	9.052	6.336×10^{3}	3.59×10^{-5}
Complex **2**	3.495×10^{-4}	1.11×10^{-3}	6.990	6.297×10^{3}	5.49×10^{-5}
Complex **3**	1.570×10^{-4}	8.68×10^{-4}	3.14	3.617×10^{3}	1.83×10^{-5}

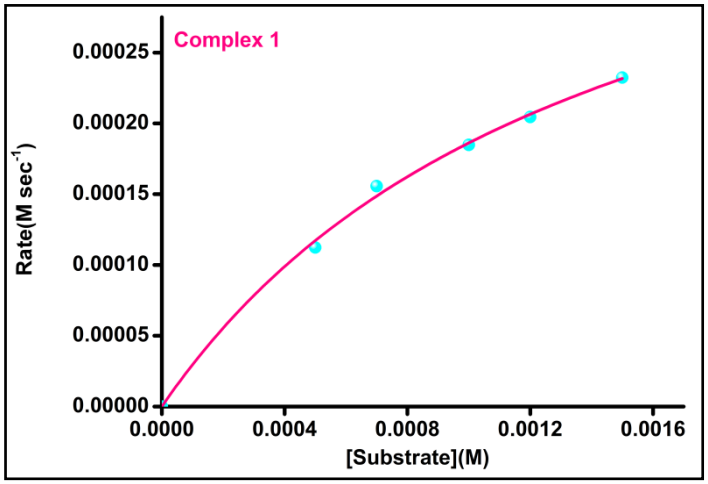

(a)

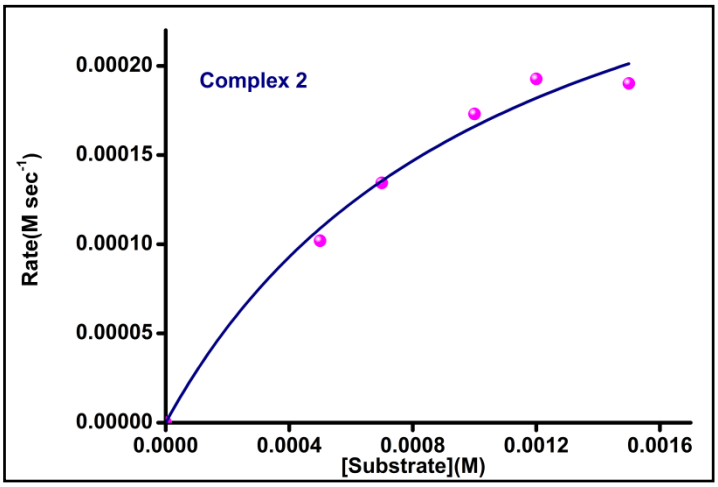

(b)

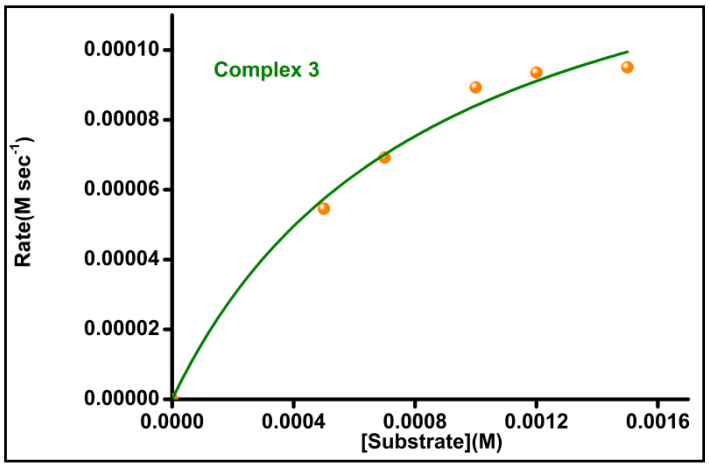

(c)

Fig. S14 Plot of enzymatic kinetics of hydrolysis of 4-NPP for (a) complex **1**, (b) complex **2** and (c) complex **3.**

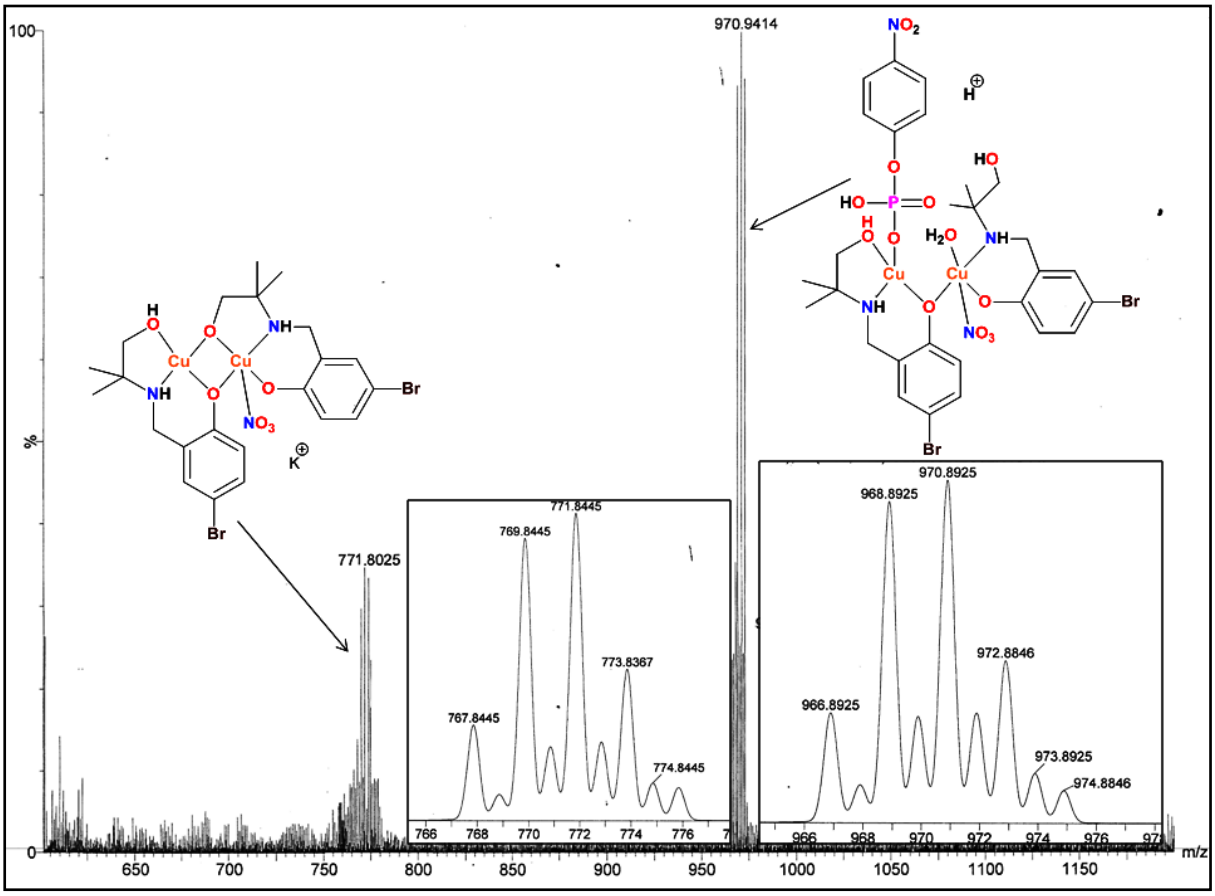

Fig. S15 ESI-MS spectrum of reaction mixture of complex **2** and 4-NPP recorded in positive mode.

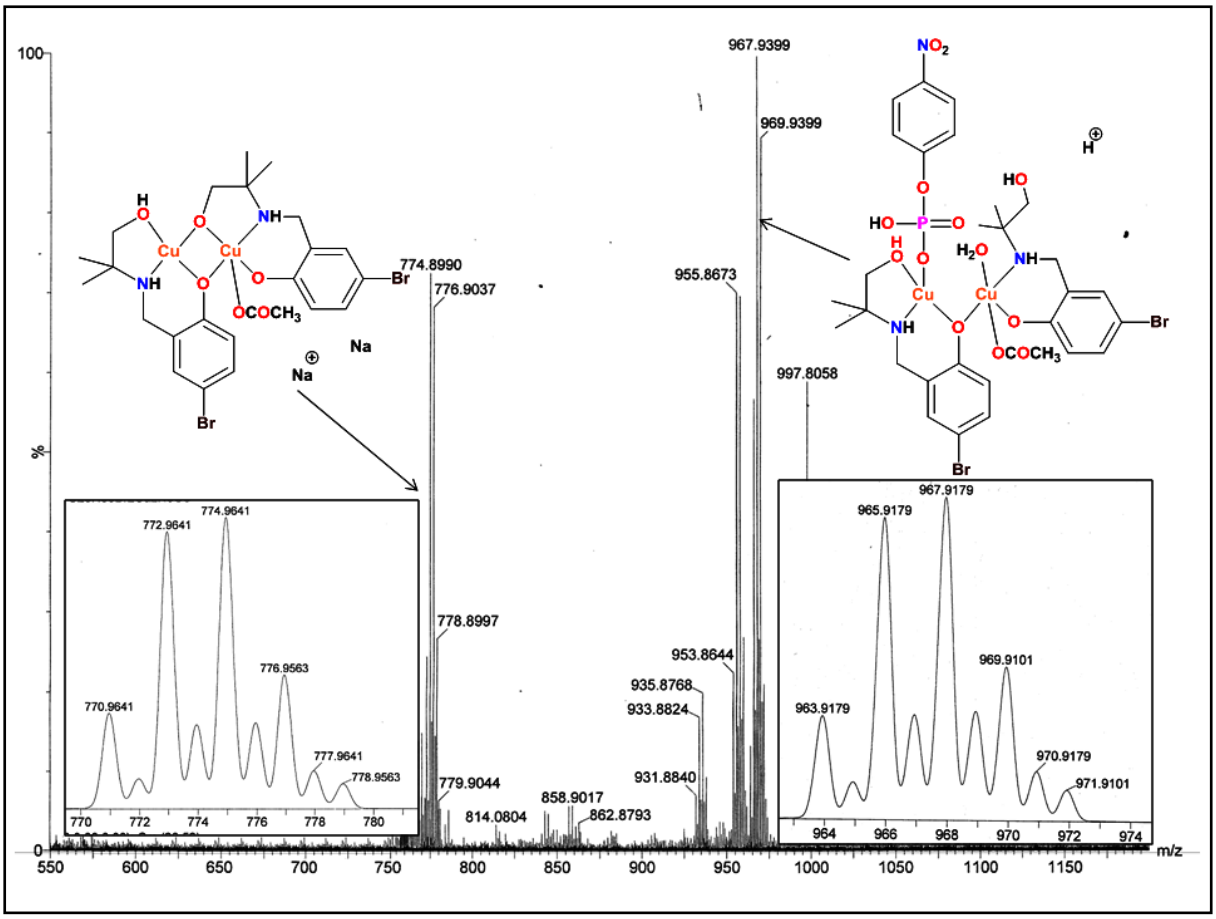

Fig. S16 ESI-MS spectrum of reaction mixture of complex **3** and 4-NPP recorded in positive mode.

Table S4 Relative Gibbs free energies in DMF solution for compounds involved in the reaction shown in the scheme 2 having symmetrically disposition of bischelate ligand L. The energy for initial complexes is arbitrarily taken to zero. All energies are in kJ/mol.

Compounds	Relative Free Energies in DMF			
	Vacant	ClO_4^-	NO_3^-	AcO^-
$[Cu_2L_2]$ (**As**) + HPO_4Ar^- + H_2O	0.0	0.0	0.0	0.0
$[Cu_2L_2(HPO_4Ar)]^-$ (**Bs**) + H_2O	-42.1	-50.6	-43.1	-39.5
$[Cu_2L_2(HPO_4Ar)(H_2O)]^-$ (**Cs**)	-85.6	-101.2	-97.0	-93.0
$[Cu_2L_2(H_2PO_4)]^-$ (**Ds**) + HOAr	-74.3	-70.6	-66.1	-72.4
$[Cu_2L_2(H_2O)]$ (**Es**) + $H_2PO_4^-$ + HOAr	-27.1	-37.2	-36.3	-34.9

Ar = $-C_6H_4NO_2$.

Table S5 Main geometric parameters for the optimized binuclear structures. Distances in

Angstroms, Angles in Degrees.

Compounds	Vacant	ClO_4^-	NO_3^-	AcO^-
$[Cu_2(L)_2]$ (**A**)				
$Cu_A \cdots Cu_B$	3.014	2.899	2.851	2.875
Cu_A- μ -O_{Alk}	1.929	1.947	1.958	1.965
Cu_A- μ -O_{Ar}	2.028	2.021	2.038	1.998
Cu_A-O_{Ar}	1.886	1.911	1.915	1.938
Cu_A-N	2.086	2.087	2.090	2.118
Cu_A-O_X	*n.a.*	2.718	2.492	2.511
Cu_B- μ -O_{Alk}	1.958	1.982	1.988	1.993
Cu_B- μ -O_{Ar}	2.008	2.050	2.065	2.330
Cu_B-O_{Alk}	1.874	1.898	1.905	1.924
Cu_B-N	2.062	2.043	2.037	2.048
Cu_B-O_X	*n.a.*	2.588	2.432	2.131
θ	161.9º	143.0º	136.8º	129.8º
$[Cu_2L_2(HPO_4Ar)]^-$ (**B**)				
$Cu_A \cdots Cu_B$	3.066	3.051	3.009	3.000
Cu_A- μ -O_{Alk}	2.012	2.011	2.007	2.005
Cu_A- μ -O_{Ar}	2.094	2.091	2.089	2.065
Cu_A-O_{Ar}	1.923	1.936	1.939	1.945
Cu_A-N	2.132	2.113	2.113	2.126
Cu_A-O_P	2.168	2.185	2.208	2.216
Cu_B- μ -O_{Alk}	2.001	2.002	2.007	2.018
Cu_B- μ -O_{Ar}	1.974	2.013	2.030	2.075
Cu_B-O_{Alk}	1.880	1.902	1.924	1.926
Cu_B-N	2.084	2.060	2.051	2.056
Cu_B-O_X	*n.a.*	2.564	2.386	2.289
θ	175.9º	159.2º	151.6º	147.1º

$[Cu_2L_2(HPO_4Ar)(H_2O)]^-$ (**C**)				
$Cu_A \cdots Cu_B$	3.066	3.033	2.984	2.974
Cu_A- μ -O_{Alk}	2.029	2.020	2.023	2.023
Cu_A- μ -O_{Ar}	2.101	2.081	2.069	2.044
Cu_A-O_{Ar}	1.923	1.928	1.932	1.944
Cu_A-N	2.138	2.111	2.108	2.123
Cu_A-O_P	2.148	2.213	2.233	2.240
Cu_B- μ -O_{Alk}	2.025	2.010	2.013	2.018
Cu_B- μ -O_{Ar}	1.963	1.991	2.020	2.082
Cu_B-O_{Alk}	1.914	1.926	1.940	1.957
Cu_B-N	2.075	2.036	2.029	2.026
Cu_B-O_X	*n.a.*	2.761	2.403	2.284
$Cu_B \cdots O_W$	2.437	3.023	3.136	3.332
θ	165.0º	157.9º	148.7º	143.3º
$[Cu_2L_2(H_2O)(HPO_4Ar)]^-$ (**C1**)				
$Cu_A \cdots Cu_B$	3.694	3.631	3.651	3.669
Cu_A- μ -O_{Alk}	2.062	1.999	1.993	1.990
Cu_A-O_W	2.036	2.039	2.036	2.031
Cu_A-O_{Ar}	1.947	1.962	1.966	1.968
Cu_A-N	2.094	2.092	2.091	2.094
Cu_A-O_P	2.254	2.293	2.303	2.312
Cu_B- μ -O_{Alk}	1.949	1.958	1.969	1.980
Cu_B-O_{Ar}	1.932	1.951	2.008	2.018
Cu_B-O_{Alk}	1.954	1.991	1.991	2.034
Cu_B-N	2.108	2.074	2.074	2.082
Cu_B-O_X	*n.a.*	2.655	2.379	2.248
$[Cu_2L(LH)(\mu\text{-}OH)(HPO_4Ar)]^-$ (**C2**)				

$Cu_A \cdots Cu_B$	2.968	2.991	3.006	2.970
Cu_A- μ -O_{Alk}	1.991	2.074	2.068	2.023
Cu_A- μ -OH	2.054	1.930	1.924	1.973
Cu_A-O_{Ar}	1.945	1.981	1.984	1.961
Cu_A-N	2.109	2.119	2.119	2.128
Cu_A-O_P	2.182	2.272	2.285	2.253
Cu_B- μ -O_{Alk}	2.022	2.023	2.014	2.059
Cu_B- μ -OH	1.951	2.282	2.329	2.007
Cu_B-O_{Ar}	1.917	1.956	1.995	2.250
Cu_B-N	2.098	2.078	2.065	2.085
Cu_B-O_X	*n.a.*	2.721	2.397	2.250
Cu_B-O_{Alk}	3.316	2.107	2.157	2.756
θ	158.9º	145.8º	144.7º	156.3º
$[Cu_2L(LH)(HO \cdots HPO_3 \cdots OAr)]^-$ (**TS**)				
$Cu_A \cdots Cu_B$	3.204	3.071	3.100	3.174
Cu_A- μ -O_{Alk}	2.272	2.057	2.057	2.064
Cu_A-OH	2.077	1.939	1.932	1.923
Cu_A-O_{Ar}	1.952	1.996	2.002	2.009
Cu_A-N	2.112	2.081	2.086	2.092
Cu_A-O_P	1.983	2.245	2.261	2.273
Cu_B- μ -O_{Alk}	1.892	1.936	1.942	1.924
Cu_B-O_{Ar}	1.926	1.961	1.985	1.920
Cu_B-O_{Alk}	2.065	2.100	2.129	2.168
Cu_B-N	2.086	2.075	2.069	2.077
Cu_B-O_X	*n.a.*	2.496	2.312	2.190
P···OH	1.796	2.286	2.338	2.379
P···OAr	2.271	1.872	1.863	1.858

$[Cu_2L(LH)(H_2PO_4\text{-}OAr)]^-$ (**C3**)				
$Cu_A\cdots Cu_B$	2.990	3.092	3.105	3.119
Cu_A-- μ -O_{Alk}	1.993	1.986	1.987	1.997
Cu_A-- μ -O_{Ar}	2.151	2.165	2.161	2.105
Cu_A-O_{Ar}	1.919	1.932	1.939	1.953
Cu_A-N	2.096	2.133	2.129	2.127
Cu_A-O_P	2.150	2.099	2.095	2.117
Cu_B- μ -O_{Alk}	1.920	1.911	1.912	1.920
Cu_B- μ -O_{Ar}	2.038	2.066	2.103	2.196
Cu_B-O_{Alk}	1.907	2.107	2.159	2.142
Cu_B-N	2.068	2.057	2.055	2.060
Cu_B-O_X	*n.a.*	2.184	2.097	2.020
θ	150.1º	176.5º	179.1º	178.6º
$[Cu_2L_2(H_2PO_4)]^-$ (**D**)				
$Cu_A\cdots Cu_B$	3.245	3.130	3.070	3.046
Cu_A- μ -O_{Alk}	2.001	1.998	1.995	1.997
Cu_A- μ -O_{Ar}	2.513	2.289	2.246	2.172
Cu_A-O_{Ar}	1.930	1.936	1.938	1.952
Cu_A-N	2.148	2.132	2.132	2.140
Cu_A-O_P	1.973	2.043	2.075	2.102
Cu_B-μ-O_{Alk}	2.006	1.990	1.991	1.994
Cu_B-μ-O_{Ar}	1.971	2.010	2.047	2.129
Cu_B-O_{Alk}	1.884	1.902	1.919	1.935
Cu_B-N	2.107	2.069	2.063	2.066
Cu_B-O_X	*n.a.*	2.716	2.405	2.257
θ	172.3º	162.7º	153.9º	148.5º
$[Cu_2L_2(H_2O)]$ (**E**)				
$Cu_A\cdots Cu_B$	3.009	2.894	2.847	2.828

Cu_A- μ -O_{Alk}	1.939	1.955	1.964	1.964
Cu_A- μ -O_{Ar}	2.037	2.023	2.035	2.023
Cu_A-O_{Ar}	1.882	1.906	1.909	1.924
Cu_A-N	2.084	2.082	2.084	2.106
Cu_A-O_X	*n.a.*	2.732	2.537	2.242
Cu_B- μ -O_{Alk}	1.964	1.988	1.992	1.975
Cu_B-μ-O_{Ar}	1.991	2.042	2.064	2.144
Cu_B-O_{Alk}	1.893	1.919	1.928	1.960
Cu_B-N	2.055	2.042	2.032	2.045
Cu_B-O_X	*n.a.*	2.455	2.345	2.465
$Cu_B\cdots O_W$	3.392	3.399	3.391	3.491
θ	159.7º	141.5º	135.2º	129.4º

Ar = -$C_6H_4NO_2$. The θ value is defined as the bent angle between CuO_2 planes in the Cu_2O_2 ring.

Table S6 Continous Shape Measures (CSM) for copper atoms in the computed geometries accross the proposed pathway.

Compounds	Vacant	ClO_4^-	NO_3^-	AcO^-
$[Cu_2(L)_2]$ (**A**)				
Cu_A	S_{SQ} = 1.01	S_{SQ} = 0.73 S_{SPY} = 3.09	S_{SQ} = 0.67 S_{SPY} = 2.35	S_{SQ} = 0.64 S_{SPY} = 2.81
Cu_B	S_{SQ} = 0.70	S_{SQ} = 1.70 S_{SPY} = 3.07 S_{TBP} = 4.10	S_{SQ} = 1.98 S_{SPY} = 3.30 S_{TBP} = 3.84	S_{TBP} = 3.66 S_{SPY} = 4.71 S_{SQ} = 4.60
$[Cu_2L_2(HPO_4Ar)]^-$ (**B**)				
Cu_A	S_{SPY} = 0.57 S_{SQ} = 1.40	S_{SPY} = 0.85 S_{SQ} = 1.73 S_{TBP} = 3.74	S_{SPY} = 0.73 S_{SQ} = 1.41 S_{TBP} = 4.15	S_{SPY} = 0.68 S_{SQ} = 1.28 S_{TBP} = 4.64
Cu_B	S_{SQ} = 1.11	S_{SQ} = 1.04 S_{SPY} = 1.40 S_{TBP} = 3.63	S_{SQ} = 1.24 S_{SPY} = 1.51 S_{TBP} = 3.40	S_{SPY} = 1.38 S_{SQ} = 1.41 S_{TBP} = 3.54

$[Cu_2L_2(HPO_4Ar)(H_2O)]^-$ (**C**)				
Cu_A	$S_{SPY} = 0.51$ $S_{SQ} = 1.36$	$S_{SPY} = 0.80$ $S_{SQ} = 1.44$ $S_{TBP} = 4.06$	$S_{SPY} = 0.64$ $S_{SQ} = 1.09$ $S_{TBP} = 4.85$	$S_{SPY} = 0.63$ $S_{SQ} = 0.97$ $S_{TBP} = 5.56$
Cu_B	$S_{SQ} = 1.21$ $S_{SPY} = 2.02$	$S_{SQ} = 1.73$ $S_{SPY} = 2.63$ $S_{TBP} = 3.33$	$S_{SQ} = 1.91$ $S_{SPY} = 2.29$ $S_{TBP} = 2.92$	$S_{SPY} = 2.45$ $S_{SQ} = 2.45$ $S_{TBP} = 2.86$
$[Cu_2L_2(H_2O)(HPO_4Ar)]^-$ (**C1**)				
Cu_A	$S_{SPY} = 1.71$ $S_{TBP} = 1.77$ $S_{SQ} = 2.28$	$S_{SPY} = 1.77$ $S_{TBP} = 1.87$ $S_{SQ} = 2.15$	$S_{TBP} = 1.76$ $S_{SPY} = 1.96$ $S_{SQ} = 2.35$	$S_{TBP} = 1.83$ $S_{SPY} = 1.92$ $S_{SQ} = 2.27$
Cu_B	$S_{SQ} = 0.33$	$S_{SQ} = 1.90$ $S_{SPY} = 2.34$ $S_{TBP} = 2.66$	$S_{SPY} = 1.84$ $S_{SQ} = 2.01$ $S_{TBP} = 2.02$	$S_{TBP} = 1.72$ $S_{SPY} = 2.20$ $S_{SQ} = 2.92$
$[Cu_2L(LH)(\mu\text{-}OH)(HPO_4Ar)]^-$ (**C2**)				
Cu_A	$S_{SPY} = 0.55$ $S_{SQ} = 1.33$ $S_{TBP} = 4.38$	$S_{SPY} = 0.30$ $S_{SQ} = 0.79$ $S_{TBP} = 5.32$	$S_{SPY} = 0.32$ $S_{SQ} = 0.76$ $S_{TBP} = 5.23$	$S_{SPY} = 0.59$ $S_{SQ} = 1.33$ $S_{TBP} = 3.87$
Cu_B	$S_{SQ} = 6.37$	$S_{SPY} = 1.32$ $S_{OCT} = 1.87$	$S_{SPY} = 0.96$ $S_{OCT} = 1.22$	$S_{SPY} = 1.15$ $S_{OCT} = 2.76$
$[Cu_2L(LH)(HO\cdots HPO_3\cdots OAr)]^-$ (**TS**)				
Cu_A	$S_{SQ} = 1.95$ $S_{SPY} = 2.53$ $S_{TBP} = 4.19$	$S_{SQ} = 1.86$ $S_{SPY} = 2.05$ $S_{TBP} = 2.73$	$S_{SQ} = 1.86$ $S_{SPY} = 2.01$ $S_{TBP} = 2.67$	$S_{SQ} = 1.93$ $S_{SPY} = 2.03$ $S_{TBP} = 2.57$
Cu_B	$S_{SQ} = 0.57$	$S_{SQ} = 0.42$ $S_{SPY} = 0.67$	$S_{SPY} = 0.49$ $S_{SQ} = 0.61$	$S_{SPY} = 0.66$ $S_{SQ} = 1.29$
$[Cu_2L(LH)(H_2PO_4\text{-}OAr)]^-$ (**C3**)				
Cu_A	$S_{SPY} = 1.76$	$S_{SPY} = 0.66$	$S_{SPY} = 0.69$	$S_{SPY} = 0.77$

	S_{TBP} = 2.47	S_{SQ} = 1.54	S_{SQ} = 1.56	S_{SQ} = 1.45
	S_{SQ} = 2.77	S_{TBP} = 5.22	S_{TBP} = 4.90	S_{TBP} = 3.91
Cu_B	S_{SQ} = 6.46	S_{TBP} = 0.76	S_{TBP} = 0.49	S_{TBP} = 0.68
		S_{SPY} = 4.27	S_{SPY} = 4.59	S_{SPY} = 4.95
$[Cu_2L_2(H_2PO_4)]^-$ (**D**)				
	S_{SPY} = 2.57	S_{SPY} = 1.19	S_{SPY} = 0.89	S_{SPY} = 0.69
Cu_A	S_{TBP} = 4.09	S_{SQ} = 2.45	S_{SQ} = 1.90	S_{SQ} = 1.50
	S_{SQ} = 4.29	S_{TBP} = 4.20	S_{TBP} = 4.70	S_{TBP} = 5.10
		S_{SQ} = 1.49	S_{SQ} = 1.61	S_{SPY} = 1.82
Cu_B	S_{SQ} = 0.39	S_{SPY} = 2.06	S_{SPY} = 1.86	S_{SQ} = 2.08
		S_{TBP} = 3.07	S_{TBP} = 2.89	S_{TBP} = 2.82
$[Cu_2L_2(H_2O)]$ (**E**)				
Cu_A	S_{SQ} = 0.99	S_{SQ} = 0.75	S_{SQ} = 0.67	S_{SQ} = 0.74
		S_{SPY} = 3.29	S_{SPY} = 2.56	S_{SPY} = 2.40
		S_{SQ} = 1.36	S_{SQ} = 1.64	S_{SQ} = 2.25
Cu_B	S_{SQ} = 0.63	S_{SPY} = 2.41	S_{SPY} = 2.62	S_{SPY} = 2.94
		S_{TBP} = 4.25	S_{TBP} = 3.92	S_{TBP} = 3.98

Continuous shape measures from ideal square-planar (S_{SQ}), square-pyramidal (S_{SPY}), trigonal-bipyramidal (S_{TBP}), or octahedral (S_{OCT}) geometries.

Ar = $-C_6H_4NO_2$.

Table S7 Crystallographic data and details of refinements for complexes **2** and **3**

	2·C_2H_5OH·0.5(H_2O)	**3**·MeCN·H_2O
CCDC Number	1835391	1835392
empirical formula	$C_{46}H_{64}Br_4Cu_4N_6O_{15.5}$	$C_{52}H_{74}Br_4Cu_4N_6O_{14}$
Fw	1522.83	1580.97
Crystal system	Monoclinic	Monoclinic
space group	$P2_1/c$	$P\ 2_1/n$
a /Å	12.401(3)	11.3423(10)
b/Å	19.901(6)	11.3744(10)
c /Å	13.776(4)	24.430(2)

α /°	90.0	90.0
β/°	107.718(5)	100.142(3)
γ /°	90.0	90.0
V/Å^3	3238.5(16)	3102.5(5)
Z	2	2
D_{calcd} /mg m^{-3}	1.562	1.692
μ (Mo-Kα) (mm^{-1})	3.823	3.993
F(000)	1524	1592
θ range (°)	1.86-25.6	1.69 -24.13
collected reflections	15198	32079
indep reflections	5700	4926
R_{int}	0.086	0.081
Obs reflecs[I> 2σ(I)]	2963	3609
Parameters	342	372
R1 [I> 2σ(I)]	0.0621	0.0444
wR2 [I> 2σ(I)]	0.1518	0.0977
GOF on F^2	0.973	1.014
residuals (e Å^{-3})	1.183, -1.319	0.670, -0.422

CCDC 1835391-1835392 contain the supplementary crystallographic data for this paper. These data can be obtained free charge from the Cambridge Crystallographic Data Centre viahttp://www.ccdc.cam.ac.uk/5 data_request/cif.